Understanding Bjerknes Compensation in Atmosphere and Ocean Heat Transports Using a Coupled Box Model

HAIJUN YANG AND YINGYING ZHAO

Laboratory for Climate and Ocean–Atmosphere Studies, and Department of Atmospheric and Oceanic Sciences, School of Physics, Peking University, Beijing, China

ZHENGYU LIU

Laboratory for Climate and Ocean–Atmosphere Studies, and Department of Atmospheric and Oceanic Sciences, School of Physics, Peking University, Beijing, China, and Department of Atmospheric and Oceanic Sciences, and Nelson Center for Climate Research, University Wisconsin–Madison, Madison, Wisconsin

(Manuscript received 21 April 2015, in final form 3 August 2015)

ABSTRACT

A coupled box model is used to study the compensation between atmosphere and ocean heat transports. An analytical solution to the Bjerknes compensation (BJC) rate, defined as the ratio of anomalous atmosphere heat transport (AHT) to anomalous ocean heat transport (OHT), is obtained. The BJC rate is determined by local feedback between surface temperature and net heat flux at the top of atmosphere (TOA) and the AHT efficiency. In a stable climate that ensures global energy conservation, the changes between AHT and OHT tend to be always out of phase, and the BJC is always valid. This can be demonstrated when the climate is perturbed by freshwater flux. The BJC in this case exhibits three different behaviors: the anomalous AHT can undercompensate, overcompensate, or perfectly compensate the anomalous OHT, depending on the local feedback. Stronger negative local feedback will result in a lower BJC rate. Stronger positive local feedback will result in a larger overcompensation. If zero climate feedback occurs in the system, the AHT will compensate the OHT perfectly. However, the BJC will fail if the climate system is perturbed by heat flux. In this case, the changes in AHT and OHT will be in phase, and their ratio will be closely related to the mean AHT and OHT. In a more realistic situation when the climate is perturbed by both heat and freshwater fluxes, whether the BJC will occur depends largely on the interplay among meridional temperature and salinity gradients and the thermohaline circulation strength. This work explicitly shows that the energy conservation is the intrinsic mechanism of BJC and establishes a specific link between radiative feedback and the degree of compensation. It also implies a close relationship between the energy balance at the TOA and the ocean thermohaline dynamics.

1. Introduction

One robust feature of the climate system is that Earth's energy balance is maintained by hemispherically antisymmetric meridional heat transports (MHTs) with peak values of about 5.5 PW (1 PW = 10^{15} W) around 35°N and 35°S (Trenberth and Caron 2001). The atmosphere heat transport (AHT) dominates in the regions poleward of about 30°N and 30°S, while the ocean heat transport (OHT) dominates in the deep tropics. Apart from the long-term mean state, the changes in AHT and OHT appear to be related to each other. Bjerknes (1964) first suggested that, if the net radiation forcing at the top of the atmosphere (TOA) and the ocean heat storage did not vary too much, the total energy transport by the climate system would not vary too much either; so any large variations in AHT and OHT should be equal in magnitude and opposite in signs. This simple scenario has become known as the Bjerknes compensation (BJC), suggesting a strong negative relationship between the changes in AHT and OHT.

The BJC has been explored widely in many studies, using models ranging from simple energy balance models (EBMs) (e.g., Lindzen and Farrell 1977; Stone 1978; North 1984; Langen and Alexeev 2007; Rose and Ferreira

Denotes Open Access content.

Corresponding author address: Haijun Yang, Department of Atmospheric and Oceanic Sciences, School of Physics, Peking University, 209 Chengfu Road, Beijing 100871, China.
E-mail: hjyang@pku.edu.cn

DOI: 10.1175/JCLI-D-15-0281.1

2013; Liu et al. 2015) to complicated general circulation models (GCMs) (e.g., Zhang and Delworth 2005; Shaffrey and Sutton 2006; Cheng et al. 2007; Van der Swaluw et al. 2007; Kang et al. 2008, 2009; Vellinga and Wu 2008; Vallis and Farneti 2009; Zhang et al. 2010; Frierson and Huang 2012; Donohoe et al. 2013; Farneti and Vallis 2013; Rose and Ferreira 2013; Yang et al. 2013; Yang and Dai 2014). Usually, the BJC is valid at decadal and longer time scales. The BJC can occur in internal climate variability (e.g., Shaffrey and Sutton 2006) and in climate responses to external forcing (e.g., Vellinga and Wu 2008; Rose and Ferreira 2013; Yang and Dai 2014). The BJC rate, defined as the ratio of anomalous AHT to anomalous OHT, has a wide range, from anomalous AHT being much smaller (or larger) than anomalous OHT to being comparable with anomalous OHT (perfect compensation), as shown in different modeling studies. Furthermore, the BJC rate can vary significantly at different latitudes (e.g., Kang et al. 2008, 2009; Vellinga and Wu 2008; Enderton and Marshall 2009; Vallis and Farneti 2009; Zhang et al. 2010; Farneti and Vallis 2013; Yang et al. 2013; Seo et al. 2014).

In spite of these studies, important questions on BJC remain, especially from a theoretical perspective. For example, what determines the BJC rate? It has long been recognized that climate feedback is important to the BJC (Stone 1978). Modeling studies have also shown that the BJC rate can change significantly with climate feedbacks, notably the cloud feedback and water vapor feedback in the tropics (e.g., Kang et al. 2008, 2009; Zhang et al. 2010; Zelinka and Hartmann 2012; Huang and Zhang 2014; Seo et al. 2014) and extratropics (e.g., Herweijer et al. 2005; Abbot and Tziperman 2008; Rose and Ferreira 2013) and the sea ice–albedo feedback at high latitudes (e.g., North 1975; Enderton and Marshall 2009). Langen and Alexeev (2007), Enderton and Marshall (2009), and Rose and Ferreira (2013) discussed briefly the effect of strength and sign of climate feedback on the BJC. However, the relationship between climate feedback and BJC needs to be studied systematically.

Our recent work (Liu et al. 2015) established a theoretical relationship between the BJC and climate feedbacks. Using the EBM of North (1975) with idealized settings, Liu et al. (2015) derived analytical solutions of the BJC with a focus on the role of climate feedback. Consistent with previous studies, these analytical solutions suggested that the BJC is usually valid in a stable climate system because of dominant negative climate feedback. The overall magnitude of the BJC rate is determined by the climate feedback. The BJC is assumed to be a "free mode" or eigenmode of a coupled climate system. Therefore, how the BJC would actually occur depends on how the climate system is perturbed. This question is explored thoroughly in this paper using a conceptual coupled box model. This coupled box model includes a four-box dynamical ocean and a two-box equilibrium atmosphere (Fig. 1). The ocean has explicit thermohaline circulation (THC) dynamics, and the atmosphere is always in equilibrium with the ocean at decadal and longer time scales.

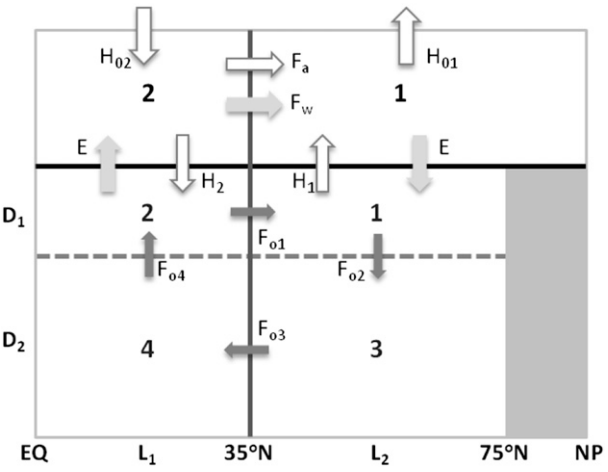

FIG. 1. Schematic plot of the coupled box model. Boxes 1 and 3 represent the upper and lower layers of extratropical ocean, and boxes 2 and 4, of the tropical ocean, respectively; D_1 and D_2 are the depths of upper and lower ocean layers, respectively; L_1 and L_2 are the meridional scales of the tropical and extratropical boxes, respectively; H_1 and H_2 are the ocean heat gains through the sea surface in the extratropics and tropics, respectively; H_{01} and H_{02} are the net energy gains at the TOA in the extratropics and tropics, respectively; E is the net freshwater loss in the tropics or the net freshwater gain in the extratropics; F_a is the meridional atmosphere energy transport; F_w is the meridional atmosphere moisture transport; and F_{o1}–F_{o4} illustrate qualitatively the heat transports among different ocean boxes.

This study focuses on equilibrium responses of the coupled box model to external forcing. First, a reasonable mean climate of the box model is determined after a brief discussion on some model parameters. The reference climate is in the regime of a stable equilibrium state with a strong (weak) meridional temperature (salinity) gradient, which resembles Earth's current climate. Second, an analytical solution to the BJC is obtained in the box model. Third, perturbation experiments are performed to investigate whether the BJC would occur. In a stable climate with global energy conservation, the changes in AHT and OHT tend to always be out of phase, and the BJC is always valid. This can be realized by perturbing the climate with freshwater flux. The BJC exhibits three different behaviors under such perturbation: the anomalous AHT can undercompensate, overcompensate, or perfectly compensate the anomalous OHT, depending on the local feedback. However, the

BJC will fail if the climate system is perturbed by anomalous heat flux. In this case, the changes in AHT and OHT will be in phase, and their ratio is closely related to the mean MHTs in both ocean and atmosphere. In a more realistic situation when the climate is perturbed by both heat and freshwater fluxes, whether the BJC will occur depends largely on the interplay among meridional temperature and salinity gradients and the THC strength.

Because of model simplicity and the lack of some complex climate dynamics, the box model can only identify the most fundamental mechanism of the BJC. Energy conservation is the intrinsic mechanism of the BJC, which forces the out-of-phase changes in AHT and OHT. The analytical solution of BJC in this work establishes a specific link between the radiative feedback and the degree of compensation, which was hinted but not clearly demonstrated in previous studies (e.g., Rose and Ferreira 2013). This link also implies a close relationship between the THC and the radiation balance at the TOA. Violation of energy conservation of climate system will result in failure of BJC, and in-phase changes in AHT and OHT. Our analytical solution also provides an easy and practical approach to scale their relative changes. This paper is organized as follows. Section 2 introduces the box model and derivation of the BJC. Section 3 investigates the BJC under different external forcing. A brief discussion and conclusions are given in section 4.

2. Coupled box model

a. Basic equations

The model consists of a four-box ocean and a two-box atmosphere (Fig. 1). The ocean component includes THC dynamics explicitly. The two-box atmosphere covers one hemisphere between the equator and 75°N, and the underlying four-box ocean spans an arbitrary longitude sector (60° for the Atlantic sector or 180° for the global Northern Hemisphere ocean). The atmosphere is assumed to mix the heat perfectly in the zonal direction and is always in quasi equilibrium with the surface ocean. All the boxes are linked at 35°N, where the zonal-mean net radiative forcing is close to zero and the northward AHT is near its peak. The zonal-mean net radiative forcing is positive (negative) south (north) of 35°N. The ocean model was based on Stommel (1961) and further developed in many studies (e.g., Marotzke 1990; Huang et al. 1992; Tziperman et al. 1994; Nakamura et al. 1994, hereinafter NSM94; Marotzke and Stone 1995, hereinafter MS95). Detailed derivations can be found in those publications. Here, we have the final forms of the equations for the four-box ocean system:

$$m_1\dot{T}_1 = \frac{1}{\epsilon c\rho_0 D_1}[(A_1 - B_1T_1) + \chi(T_2 - T_1)] + q(T_2 - T_1), \tag{1a}$$

$$m_2\dot{T}_2 = \frac{1}{\epsilon c\rho_0 D_1}[(A_2 - B_2T_2) - \chi(T_2 - T_1)] + q(T_4 - T_2), \tag{1b}$$

$$m_3\dot{T}_3 = q(T_1 - T_3), \tag{1c}$$

$$m_4\dot{T}_4 = q(T_3 - T_4), \tag{1d}$$

$$m_1\dot{S}_1 = -\frac{S_0}{\epsilon_w D_1}\gamma(T_2 - T_1) + q(S_2 - S_1), \tag{2a}$$

$$m_2\dot{S}_2 = +\frac{S_0}{\epsilon_w D_1}\gamma(T_2 - T_1) + q(S_4 - S_2), \tag{2b}$$

$$m_3\dot{S}_3 = q(S_1 - S_3), \quad \text{and} \tag{2c}$$

$$m_4\dot{S}_4 = q(S_3 - S_4), \tag{2d}$$

where A_1 (<0) and A_2 (>0) are net incoming radiation ($\mathrm{W\,m^{-2}}$) at high and low latitudes, respectively; B_1 and B_2 are climate feedback parameters at high and low latitudes, respectively; χ and γ are the efficiencies of atmosphere heat and moisture transports; c is the seawater specific heat capacity; ρ_0 is the seawater density; S_0 is a constant reference salinity (35 psu). Relative ocean coverage in both high- and low-latitude areas is indicated by $\epsilon = G_1/G_{01} = G_2/G_{02}$; here, G_{01} and G_{02} are the entire areas of the two atmosphere boxes separated by 35°N; and G_1 and G_2 are the areas of corresponding ocean boxes. For simplicity, we assume $G_1 = G_{01}$ and $G_2 = G_{02}$. If an aquaplanet is studied, then $\epsilon = 1$; otherwise $\epsilon < 1$. The ratio of ocean and catchment area to G_{01} is given by $\epsilon_w \equiv G_1'/G_{01}$, where G_1' denotes the ocean and catchment area of the ocean basin, which includes the influence of river runoff on the oceanic freshwater budget, and it is obvious that $G_1' > G_1$. The ratio of each ocean-box volume with respect to box 1 is depicted by m_i; that is, $m_1 = 1$, $m_2 = L_1/L_2$, $m_3 = D_2/D_1$, and $m_4 = L_1D_2/(L_2D_1)$. All parameters used in this study are listed in Table 1 and are based on previous box-model studies (NSM94; MS95) and coupled model simulations (Yang et al. 2015), as well as observations (Rayner et al. 2003; Carton and Giese 2008).

The volume transport resulting from the THC between two adjacent ocean boxes q is assumed to be linearly proportional to the density difference between two surface boxes 1 and 2 (NSM94):

$$q = \kappa[\alpha(T_2 - T_1) - \beta(S_2 - S_1)] = \kappa(\alpha T_s - \beta S_s), \tag{3}$$

where κ is a constant parameter that sets the reference flushing (turnover) time scale for a surface ocean box ($\mathrm{s^{-1}}$); α and β are the thermal and haline expansion

TABLE 1. Parameters used in this study.

Symbol	Physical meaning	Value	Reference	Notes
A_1	Net incoming radiative at box 1 and 2	$-40\,\mathrm{W\,m^{-2}}$	MS95	—
A_2		$90\,\mathrm{W\,m^{-2}}$		
B_1	Local climate feedback parameter in boxes 1 and 2	$1.7\,\mathrm{W\,m^{-2}\,K^{-1}}$	MS95	—
B_2		$1.7\,\mathrm{W\,m^{-2}\,K^{-1}}$	NSM94	
$c\rho_0$	Heat capacity of a unit water volume	$4\times10^{6}\,\mathrm{J\,m^{-3}\,K^{-1}}$	MS95	—
D_1	Depth of upper and lower boxes	400 m	—	—
D_2		4000 m		
G_{01}	Entire surface area north of the dividing latitude	$1.25\times10^{14}\,\mathrm{m^2}$	MS95	—
L_1	Meridional scale of low- and high-latitude boxes	35°	MS95	—
L_2		40°		
S_0	Reference salinity	35.0 psu	MS95	—
α	Thermal expansion coefficient	$2.5\times10^{-4}\,\mathrm{K^{-1}}$	—	—
β	Haline contraction coefficient	$7.5\times10^{-4}\,\mathrm{psu^{-1}}$	—	—
ϵ	Ratio of ocean area of box 1 to G_{01} (i.e., G_1/G_{01}), $\epsilon \le 1$	0.2	MS95	Atlantic sector
ϵ_w	Ratio of ocean and catchment area to G_{01}, $\epsilon \le \epsilon_w \le 1$	0.3	MS95	—
κ	Advective time-scale coefficient	$1.2\times10^{-7}\,\mathrm{s^{-1}}$	—	$D = 5$ km
γ	Atmosphere moisture transport efficiency	$1.2\times10^{-10}\,\mathrm{m\,s^{-1}\,K^{-1}}$	MS95	Factor of 1–3
χ	Atmosphere heat transport efficiency	$1.3\,\mathrm{W\,m^{-2}\,K^{-1}}$	MS95	—

coefficients of seawater, respectively. This simple relationship for q is supported by many ocean general circulation modeling studies (e.g., Hughes and Weaver 1994). In this study, we focus on a positive (northward) meridional mass transport ($q > 0$), which assumes a temperature-dominated circulation ($\alpha T_s > \beta S_s$) and is driven by the cooling and sinking in the extratropical (northern) box and heating in the tropical box.

The meridional atmosphere and ocean heat transports are parameterized as follows:

$$F_a = \chi G_{01}(T_2 - T_1) \quad \text{and} \tag{4}$$

$$F_o = c\rho_0 \epsilon G_{01} D_1 q (T_2 - T_3). \tag{5}$$

In Eq. (1), a simple parameterization of the net radiative forcing ($\mathrm{W\,m^{-2}}$) at the TOA is used, which is widely employed in EBMs (e.g., North 1975; Wang and Stone 1980; NSM94):

$$H_{01} = A_1 - B_1 T_1 \quad \text{and} \quad H_{02} = A_2 - B_2 T_2. \tag{6}$$

The surface heat fluxes combining the AHT and the net radiation flux at the TOA are

$$H_1 = \frac{1}{\epsilon c\rho_0 D_1}[(A_1 - B_1 T_1) + \chi(T_2 - T_1)] \quad \text{and} \tag{7a}$$

$$H_2 = \frac{1}{\epsilon c\rho_0 D_1}[(A_2 - B_2 T_2) - \chi(T_2 - T_1)]. \tag{7b}$$

The spatially averaged ocean heat uptake is

$$\begin{aligned} H_1 + H_2 &= \frac{1}{\epsilon c\rho_0 D_1}(H_{01} + H_{02}) \\ &= \frac{1}{\epsilon c\rho_0 D_1}(A_1 + A_2 - B_1 T_1 - B_2 T_2), \end{aligned} \tag{8}$$

which is independent of the AHT. The oceanic heat budget, as a whole, is only determined by the net radiative forcing at the TOA:

$$\begin{aligned} m_1\dot{T}_1 + m_2\dot{T}_2 + m_3\dot{T}_3 + m_4\dot{T}_4 &= H_1 + H_2 \\ &= \frac{1}{\epsilon c\rho_0 D_1}(H_{01} + H_{02}). \end{aligned} \tag{9}$$

For a steady state, the total energy in the coupled box model is conserved. Equation (9) then becomes

$$H_1 + H_2 = H_{01} + H_{02} = 0, \tag{10}$$

which depicts that the ocean heat uptake in the tropical box is equal to the ocean heat release in the extratropical box; in other words, the energy gain in the tropical atmosphere–ocean system is equal to the energy loss in the extratropics.

For Eqs. (1) and (2), we also use the simplest assumptions that the meridional heat and moisture transports are linearly proportional to the meridional temperature gradient T_s (Budyko 1969). This Budyko-type model is widely used in EBMs (e.g., North 1975, 1984; Lindzen and Farrell 1977; Stone and Yao 1990) and is more straightforward for interpreting model physics. The atmosphere moisture transport F_w is similarly given by

$$F_w = \gamma G_{01}(T_2 - T_1), \tag{11}$$

which must be balanced by the net freshwater loss (gain) E at low (high) latitudes. Therefore,

$$E = \frac{1}{\epsilon_w G_{01}} F_w = \frac{\gamma}{\epsilon_w}(T_2 - T_1). \tag{12}$$

TABLE 2. Properties of the reference mean climate based on the parameters in Table 1. The T_s, and S_s based on CESM (Yang et al. 2015) and SODA (Carton and Giese 2008) are also listed here for references.

Variable	Physical meaning	Value	Notes
T_s	Meridional temperature contrast $T_2 - T_1$	27.4°C	This study
		27.3°C	CESM
		25.9°C	SODA
S_s	Meridional salinity contrast $S_2 - S_1$	1.4 psu	This study
		1.3 psu	CESM
		1.8 psu	SODA
T_1, T_2, T_3, and T_4	Temperature for boxes 1–4	1.0°, 28.4°, 1.0°, and 1.0°C	—
S_1, S_2, S_3, and S_4	Salinity for boxes 1–4	31.9, 33.3, 31.9, and 31.9 psu	Initial value dependent
q	Meridional ocean mass transport	6.98 Sv	—
F_w	Atmosphere moisture transport	0.41 Sv	—
F_a	Atmosphere heat transport	4.45 PW	—
F_o	Ocean heat transport	0.76 PW	—
F_t	Total meridional heat transport	5.21 PW	—

Without external freshwater sources, the total salt content of the model ocean is conserved:

$$m_1\dot{S}_1 + m_2\dot{S}_2 + m_3\dot{S}_3 + m_4\dot{S}_4 = 0. \tag{13}$$

b. Equilibrium solutions

The equilibrium states of temperature and salinity, as well as AHT and OHT, can be obtained by letting the temporal tendency be zero ($\dot{T}_i = 0$ and $\dot{S}_i = 0$):

$$B_1T_1 + B_2T_2 = A_1 + A_2, \tag{14a}$$

$$T_1 = T_3 = T_4, \quad \text{and} \tag{14b}$$

$$S_1 = S_3 = S_4 \tag{14c}$$

and

$$F_o = G_{01}(H_{02} - \chi T_s), \tag{15a}$$

$$F_a = \chi G_{01} T_s, \quad \text{and} \tag{15b}$$

$$F_t = F_o + F_a = G_{01}H_{02} = -G_{01}H_{01}. \tag{15c}$$

For reasonable values of A_1, A_2, B_1, and B_2 (Table 1), the mean surface temperature is about 15°C. Using the parameters in Table 1, the mean climate can be determined (Table 2), which is tuned to be consistent with the solutions in NSM94 and MS95 and also consistent with observations [such as HadISST (Rayner et al. 2003) and SODA (Carton and Giese 2008)] and coupled climate model results [such as CESM (Yang et al. 2015)]. The equilibrium temperatures are independent of their initial values (figure not shown) and are only related to A_i and B_i, as suggested by Eq. (14a). Therefore, the equilibrium heat and mass transports are also independent of initial conditions. The equilibrium salinity values, however, depend on their initial values because different initial values of S_i represent different amounts of freshwater. However, the salinity gradient S_s is independent of initial salinity values.

c. Bjerknes compensation

To derive the analytical solution to the BJC, let us assume a perturbation in the system. Equation (14a) suggests a relationship of the equilibrium temperature changes between two surface ocean boxes:

$$B_1\Delta T_1 = -B_2\Delta T_2 = -\frac{B_1B_2}{B_1 + B_2}\Delta T_s, \tag{16}$$

where $\Delta T_s = \Delta T_2 - \Delta T_1$. The changes in heat transport components can be obtained from Eq. (15):

$$\Delta F_o = -G_{01}(B_2\Delta T_2 + \chi\Delta T_s) = -G_{01}\Delta T_s\frac{B_1B_2 + (B_1 + B_2)\chi}{B_1 + B_2}, \tag{17a}$$

$$\Delta F_a = \chi G_{01}\Delta T_s, \quad \text{and} \tag{17b}$$

$$\Delta F_t = -G_{01}\Delta T_s\frac{B_1B_2}{B_1 + B_2}. \tag{17c}$$

The BJC rate C_R is therefore defined similar to those in Van der Swaluw et al. (2007) and in Rose and Ferreira (2013):

$$C_R \equiv \frac{\Delta F_a}{\Delta F_o} = -\frac{(B_1 + B_2)\chi}{B_1B_2 + (B_1 + B_2)\chi}. \tag{18}$$

Equation (18) states that C_R is independent of the mean climate, changes in T_s and S_s, and the heat transports themselves. It is determined by only two climate parameters: the local climate feedback B_i and the AHT coefficient χ. If we assume $B_1 = B_2 = B$, Eq. (18) can be further reduced to

$$C_R = -\frac{2\chi}{B + 2\chi} = -\frac{1}{1 + B/2\chi}. \tag{19}$$

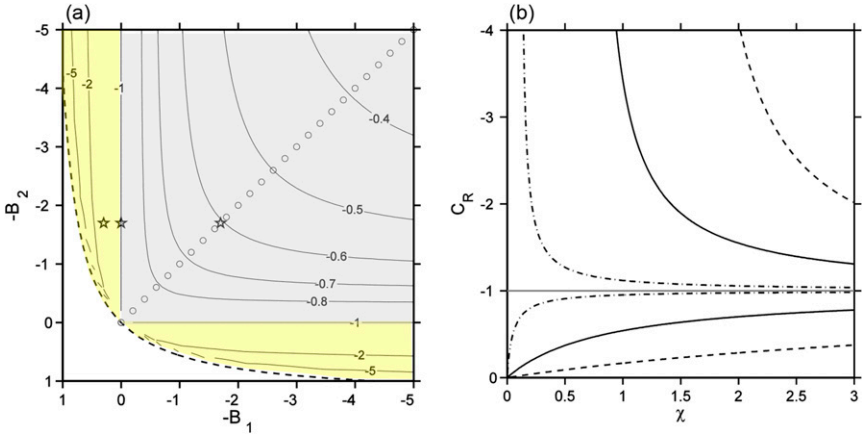

FIG. 2. (a) BJC rate C_R under the stability condition of Eq. (21) (dashed curve) with respect to the local climate feedback parameters B_1 and B_2. The atmosphere heat transport efficiency $\chi = 1.3$. Open circles show C_R when $B_1 = B_2$; stars show C_R for the cases with both local climate feedbacks negative (FB1; $-B_1 = -1.7$, $-B_2 = -1.7$), one local feedback is zero (FB2; $-B_1 = 0$, $-B_2 = -1.7$), and one local feedback is positive (FB3; $-B_1 = 0.3$, $-B_2 = -1.7$) . The shaded regions show undercompensation (gray) and overcompensation (yellow). (b) BJC rate C_R with respect to the atmosphere heat transport efficiency χ. From the bottom to the top, the seven curves are for $-B_1 = -10$, -1.7, -0.1, 0, 0.1, 0.5, and 0.8 and $-B_2 = -10$, -1.7, -0.1, -1.7, -1.7, -1.7, and -1.7.

For a stable climate with an overall negative feedback ($-B < 0$), $C_R < 0$, showing that the changes in AHT and OHT always tend to compensate each other. It is actually the nondimensional ratio B/χ that determines the BJC rate. This has been noted in the studies using one-dimensional EBMs (e.g., Lindzen and Farrell 1977; Stone 1978; North 1984). Here, we explicitly show that B/χ determines the relative changes in OHT and AHT.

It should be emphasized that C_R is always negative for a stable climate system with total energy conservation. The local climate feedback B_i must be in a reasonable range to maintain the stability of the coupled box model. This requires an overall negative feedback first:

$$-(B_1 + B_2) < 0, \tag{20}$$

and further satisfaction of the stability condition (see details in Liu et al. 2015):

$$-(B_1 + B_2) < B_1 B_2/\chi. \tag{21}$$

In fact, Eqs. (18) and (19) suggest that the changes in AHT and OHT can be undercompensated, perfectly compensated, or overcompensated, depending on how the heat efficiency B/χ is set, or more specifically, how the local climate feedback B is set, because χ is always positive and less uncertain, while B is spatial–temporal dependent and could include various positive or negative feedback processes. Stronger negative feedback B will result in lower C_R. Figure 2a shows the C_R pattern in the parameter space ($-B_1$, $-B_2$) based on Eq. (18), in which the AHT efficiency $\chi = 1.3$. The open circles show C_R when $B_1 = B_2$. The dashed curve shows the stability condition Eq. (21). Strong climate feedback (both positive and negative) means that even small surface temperature perturbation can cause big change in energy flux at the TOA based on Eq. (6), which suggests a serious violation of local energy conservation. Therefore, C_R will deviate significantly from 1. In fact, if both local feedbacks are negative, C_R will always be less than 1 (Fig. 2a, gray shaded region). The AHT change will undercompensate the OHT change, no matter how efficiently the AHT responds to the meridional temperature gradient. If either of the local feedbacks is zero, the AHT change will perfectly compensate the OHT change. If, however, a positive climate feedback arises somewhere for some reason, no matter how small it is, the AHT change will overcompensate the OHT change (Fig. 2a, yellow shaded region). Mathematically, these situations are depicted by

$$|C_R| \sim \begin{cases} <1, & \text{if} \quad B_1 B_2 > 0 \quad \text{for undercompensation} \\ =1, & \text{if} \quad B_1 B_2 = 0 \quad \text{for full compensation} \\ >1, & \text{if} \quad B_1 B_2 < 0 \quad \text{for overcompensation} \end{cases}. \tag{22}$$

The BJC rate C_R with respect to χ is shown in Fig. 2b. In the case of global negative feedback, bigger χ will result in stronger AHT and thus a better C_R. In the case of one local feedback being zero, $C_R = 1$ and is independent of χ. The local energy conservation requires the perfect BJC, regardless of the AHT efficiency. In the

case of one local feedback being positive, C_R is inversely proportional to χ. Bigger χ restrains the extent of overcompensation, because stronger AHT (because of larger χ) is more efficient to smooth out local runaway changes, reducing T_s and therefore the AHT change. In any case, a highly efficient AHT leads to a better compensation, which approaches monotonically the asymptotic line of $C_R = 1$ (Fig. 2b). A linear regression method was used to estimate χ in Yang et al. (2015), using outputs from a coupled model of a 21 000-yr simulation. They found that χ during the past 21 000 yr was about $1.5 \pm 0.1\,\mathrm{W\,m^{-2}\,K^{-1}}$, which is actually a very stable parameter in the climate system. So, in the next section we will focus on discussion of C_R with respect to climate feedback parameters.

Finally, for the convenience of later discussion, the equilibrium temperature changes can be rewritten in terms of ΔF_o as follows:

$$\Delta T_1 = \frac{B_2 \Delta F_o / G_{01}}{B_1 B_2 + (B_1 + B_2)\chi} \quad \text{and}$$
$$\Delta T_2 = \frac{-B_1 \Delta F_o / G_{01}}{B_1 B_2 + (B_1 + B_2)\chi}. \tag{23}$$

The responses of global mean temperature $T_m = (T_1 + T_2)/2$ and T_s are

$$\Delta T_m = \frac{-(B_1 - B_2)\Delta F_o / 2G_{01}}{B_1 B_2 + (B_1 + B_2)\chi} \quad \text{and}$$
$$\Delta T_s = \frac{-(B_1 + B_2)\Delta F_o / G_{01}}{B_1 B_2 + (B_1 + B_2)\chi}. \tag{24}$$

d. A brief discussion on local climate feedbacks

The local feedbacks are usually negative: that is, $-B_i \le 0$, because of the dominant negative feedback between temperature and outgoing longwave radiation (OLR) (NSM94; Zhang et al. 1994; MS95; Soden et al. 2004). However, the feedback may not be restricted to be negative everywhere. Physically, local feedbacks could become positive under extreme scenarios: for example, the strong positive feedback from water vapor in the deep tropics (Pierrehumbert 1995) and cloud radiative forcing from the stratus clouds in the subtropics (Philander et al. 1996; Clement et al. 2009). The climate system can remain stable in the presence of a weak local positive feedback (e.g., $-B_2 > 0$), because the atmosphere can transport the extra energy to the other box. In this study, B_i is generalized and can be thought of as including all the local feedbacks: the temperature feedback, the water vapor feedback, the surface albedo feedback, and the cloud feedback.

Linear regression can be used to determine the feedback parameters (B_1, B_2) based on Eq. (6) (e.g., Rose and Marshall 2009). In Yang et al. (2015), the model output from a 21 000-yr transient simulation was used to estimate B_1 and B_2. Their results showed a weak positive feedback ($-B_1 = 0.4$) in the extratropics and a strong negative feedback in the tropics ($-B_2 = -1.7$). The positive feedback was mainly due to the strong positive feedback between shortwave radiation and surface temperature, which overcame the strong negative feedback between the OLR and surface temperature. The tropical negative feedback was mainly due to the strong negative feedback between the OLR and surface temperature (in association with high clouds), which dominated the positive feedback between shortwave radiation and surface temperature.

The issues regarding climate feedbacks and sensitivities are extremely complicated and have been studied extensively by many researchers (e.g., Bates 1999, 2007, 2012; Hwang and Frierson 2010; Hwang et al. 2011). Local feedback strength determines atmosphere behaviors to a great extent, such as how the AHT will respond to surface temperature change. The relationship between local feedback strength and AHT has been studied by Hwang and Frierson (2010), Hwang et al. (2011), Zelinka and Hartmann (2011), Feldl and Roe (2013a,b), and Huang and Zhang (2014). Rose et al. (2014) explicitly showed how the AHT responded to prescribed patterns of surface heat flux (analogous to OHT in equilibrium) in different feedback regimes using both a simple EBM and a GCM. Here, we do not investigate how the local climate feedbacks can be identified correctly; instead, we want to understand conceptually the relationship between AHT and OHT (C_R), given the signs of each feedback (positive or negative) and their approximate strengths.

3. Perturbation experiments

To understand the dynamics of BJC, perturbation experiments are performed. Our focus is on the model's climate responses to external forcing, such as freshwater change due to sea ice melting or formation, and the net radiation flux change at the TOA. In the coupled box model, water hosing to the ocean does not change the energy budget, which satisfies the prerequisite to the BJC, as noted by Bjerknes (1964). Perturbing the net radiation flux at the TOA can mimic the effect of solar radiation change, planetary albedo change (e.g., change due to sea ice), and longwave radiation change due to greenhouse gases or water vapor. It should be born in mind that perturbing A or B would cause energy

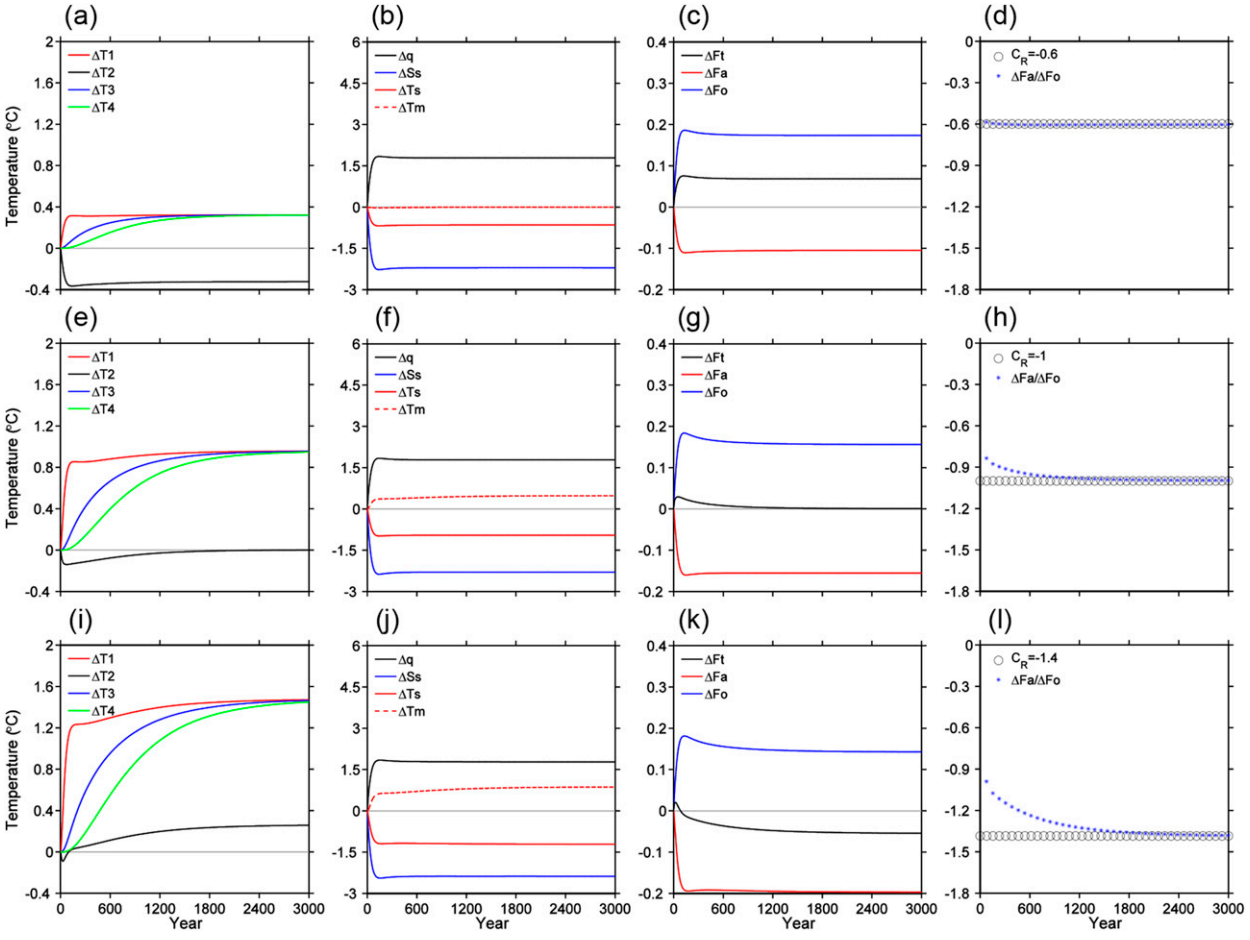

FIG. 3. Climate changes in response to freshwater removal of 0.5 Sv in ocean box 1: (a) for T (°C); (b) for q (Sv), T_m (°C), T_s (°C), and S_s (psu); and (c) for heat transport (PW); (d) the BJC rate from the model (blue asterisks) and Eq. (18) (open circles). In (a)–(d) the local climate feedbacks are both negative (FB1 case), and the mean climate listed in Table 2 is removed. (e)–(h) As in (a)–(d), but for the FB2 case. (i)–(l) As in (a)–(d), but for the FB3 case.

imbalance both globally and locally. Whether the BJC is still valid is the question to be explored here.

a. Freshwater perturbation

Figure 3 shows the model climate change when 0.5-Sv ($1\,\text{Sv} \equiv 10^6\,\text{m}^3\,\text{s}^{-1}$) freshwater is removed from the extratropical ocean box, which is accomplished by adding a positive salinity tendency ($h = 1.75 \times 10^{-9}\,\text{psu}\,\text{s}^{-1}$) in Eq. (2a). Changes in the box-model climate are obtained by subtracting the equilibrium state listed in Table 2. Since the freshwater perturbation does not affect the energy balance of the climate system, Eq. (18) is valid. The BJC exhibits three behaviors, depending on the local climate feedback as suggested by Eq. (22).

1) UNDERCOMPENSATION

Given negative climate feedbacks in both surface boxes ($-B_1 = -B_2 = -1.7$), $C_R \approx -0.6$. Figure 3d shows clearly that the model C_R reaches the analytical value quickly. The AHT change undercompensates the OHT change in this situation.

It is straightforward that removing the freshwater from the extratropical ocean box immediately increases the salinity locally ($\Delta S_1 > 0$), resulting in an enhancement of the THC ($\Delta q > 0$), which in turn transports more heat poleward ($\Delta F_o > 0$) and results in warming (cooling) in the extratropics (tropics) ($\Delta T_1 > 0$ and $\Delta T_2 < 0$); this leads to reduced meridional temperature gradient ($\Delta T_s < 0$). The atmosphere responds to the reduced ΔT_s with a weakened AHT ($\Delta F_a < 0$). The overall ocean temperature is warmer, but the overall surface temperature is unchanged ($\Delta T_m = 0$) because $B_1 = B_2$. These responses can be readily deduced from Eqs. (16), (17), (23), and (24). They are clearly shown in Figs. 3a–d. These processes have also been investigated extensively in studies using the simplest EBMs (e.g., Liu et al. 2015). The

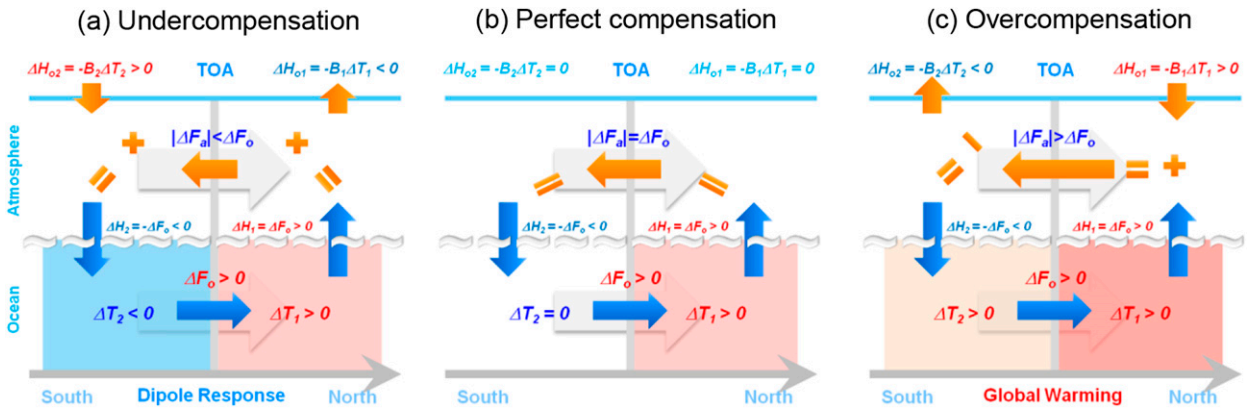

FIG. 4. Schematic diagram showing the BJC mechanism. (a) Under negative feedbacks in both extratropical and tropical boxes ($B_1B_2 > 0$), the anomalous AHT undercompensates the anomalous OHT to keep the energy conserved in both tropical and extratropical boxes. Large gray arrows denote mean heat transports. (b) Under a zero feedback in the extratropical box ($-B_1 = 0$, $B_2 \neq 0$), the anomalous AHT compensates the anomalous OHT perfectly. (c) Under a weak positive feedback in the extratropical box ($-B_1 > 0$, $B_1B_2 < 0$), the anomalous AHT has to overcompensate the anomalous OHT.

dipole-like response of extratropical warming ($\Delta T_1 > 0$) and tropical cooling ($\Delta T_2 < 0$) (Fig. 3a) is consistent with many water-hosing experiments in coupled models (e.g., Manabe and Stouffer 1995; Stouffer et al. 2007). In general, we see a stable climate with a weaker meridional temperature gradient because of the enhanced THC.

Now, let us come back to the main purpose of this study: that is, to identify the fundamental mechanism of the BJC. The tropical cooling decreases the OLR at the TOA because of negative feedback ($-B_2 < 0$), resulting in an increase of net downward energy influx ($\Delta H_{02} = -B_2\Delta T_2 > 0$). Therefore, the tropical energy loss resulting from the horizontal OHT can be partially compensated by energy gain at the TOA in the vertical direction. In other words, the tropical atmosphere does not have to import all energy from the extratropics to compensate the oceanic heat export ($|\Delta F_a| = |\Delta F_o - B_1T_1| < \Delta F_o$), leading to the undercompensation. Meanwhile, the extratropical warming increases the heat loss at the TOA because of negative feedback ($-B_1 < 0$). This reduces the downward energy influx at the TOA ($\Delta H_{01} = -B_1\Delta T_1 < 0$). Thus, the extratropical atmosphere does not have to export all extra energy to the tropical box. The fact that equal amounts of TOA flux change with opposite signs in the tropics and extratropics assures the same AHT change should satisfy the atmosphere energy balance in both tropics and extratropics. Quantitatively, as the negative feedback intensifies (larger $|B_i|$), the energy balance tends to be fulfilled more locally, instead of by horizontal redistribution; therefore, C_R decreases further, as shown in Fig. 2. It is shown clearly here that the energy conservation requires compensating changes in AHT and OHT, and the climate feedback determines the extent of compensation. This mechanism is illustrated in Fig. 4a.

2) FULL COMPENSATION

In the absence of climate feedback, full compensation will be achieved. Indeed, when $B_1B_2 = 0$, $C_R = -1$, indicating that anomalous AHT exactly compensates the anomalous OHT ($\Delta F_a = -\Delta F_o$) and that the combined heat transport in the atmosphere and ocean remains unchanged ($\Delta F_t = 0$). Figure 3h shows that the model C_R approaches 1 monotonically. It takes a longer time to reach the equilibrium than in the undercompensation case (Fig. 3d).

The full compensation only requires zero feedback locally in one box. Figures 3e–h show the climate changes with $-B_1 = 0$ and $-B_2 = -1.7$. As in the undercompensation case, the temperature response shows extratropical warming $\Delta T_1 > 0$ (Fig. 3e) for enhanced THC ($\Delta q > 0$ and $\Delta F_o > 0$) (Figs. 3f,g). However, no change occurs in the tropical temperature; that is, $\Delta T_2 = -(B_1/B_2)\Delta T_1 = 0$ because $B_1 = 0$ (Fig. 3e). Therefore, regardless of the feedback B_2 in the tropics, there is no change in the TOA energy flux of both regions (i.e., $\Delta H_{01} = -B_1\Delta T_1 = 0$ and $\Delta H_{02} = -B_2\Delta T_2 = 0$). The ocean heat gain in the extratropics has to be completely exported to the tropical atmosphere, supplying the exact heat loss in the tropical ocean due to enhanced poleward OHT [viz., $\Delta F_a = -\Delta F_o$ (Fig. 3g)], leading to full compensation (Fig. 3h). This mechanism is illustrated in Fig. 4b.

The full compensation was discussed in Rose and Ferreira (2013). This case corresponds to a stable climate with a warmer global mean temperature ($\Delta T_m = \Delta T_1/2 > 0$) (Fig. 3f) and a weaker meridional temperature gradient ($\Delta T_s < 0$). This is an ''equable'' climate (Huber and Caballero 2011; Rose and Ferreira 2013). Rose and Ferreira (2013) studied the equable climate and

found that polar warming can be achieved without any change in the TOA radiative balance. Because "the increase in OLR associated with the warming pole is exactly balanced by the reduction in OLR associated with the enhanced greenhouse," the increase in poleward OHT is exactly balanced by a reduction in AHT associated with the weaker ΔT_s (Rose and Ferreira 2013, p. 2130). This is exactly the case we discuss here. In fact, the local feedback B_i in our study is generalized. It includes all the local feedbacks: the temperature feedback, the water vapor feedback, the surface albedo feedback, and the cloud feedback. Zero gross local feedback (e.g., $B_1 = 0$) could be achieved by having different competing feedbacks.

The full compensation can also be achieved if the tropical climate feedback is zero ($B_2 = 0$). In this case, the climate has a colder global mean temperature ($\Delta T_m = \Delta T_2/2 = -(\Delta F_o/G_{01})/2\chi < 0$) in response to the same freshwater removal in the extratropical ocean (figure not shown). The zero B_2 excludes the possibility of having any net radiation change at the TOA; so the energy loss in the tropics has to be fully made up by the energy import by the atmosphere from the extratropics. This situation is plausible because of the strong positive feedback from water vapor in the deep tropics (Pierrehumbert 1995) and cloud radiative forcing from, for example, the stratus clouds in the subtropics (Philander et al. 1996; Clement et al. 2009).

3) OVERCOMPENSATION

If positive local feedback occurs somewhere, then C_R will be larger than 1. The positive feedback has to be weak because of the constraint of the stability condition Eq. (21) (Fig. 2). Figure 3l shows that $C_R = -1.4$ when $-B_1 = 0.3$ and $-B_2 = -1.7$. In this case, a stable climate is still possible in response to the external freshwater forcing, but it takes a much longer time than in the previous two cases to reach the equilibrium.

Again, the increased poleward OHT (Fig. 3k) leads to extratropical warming (Fig. 3i). However, because of the local positive feedback, the extratropical warming increases the heat gain at the TOA ($\Delta H_{01} = -B_1\Delta T_1 > 0$). (This is in analogy to the sea ice–albedo and SST positive feedback.) The extratropical atmosphere has to export more energy than that gained by the ocean to maintain the local energy balance $|\Delta F_a| = |\Delta F_o - B_1\Delta T_1| > \Delta F_o$, leading to an overcompensation (Fig. 3l). The combined energy transport ΔF_t has the same direction as the atmospheric ΔF_a (Fig. 3k). Despite increased poleward OHT, a warmer tropics occurs ($\Delta T_2 \sim -B_1\Delta F_o > 0$) (Fig. 3i) because of extra import of the atmospheric energy from the extratropics. This tropical warming increases energy loss at the TOA ($\Delta H_{02} = -B_2\Delta T_2 < 0$) and therefore can offset the extra heat gain in the extratropics. In this case, the increased poleward OHT leads to warming everywhere and thus global warming (Fig. 3i). This mechanism is illustrated in Fig. 4c.

b. Heat perturbation

It is not straightforward if the BJC is valid when the climate system is perturbed by external heating, because such perturbation can cause energy imbalance in the system. Heat perturbation experiments can be achieved by adding a temperature tendency in Eqs. (1a) and/or (1b). Slightly different from Eq. (14), the equilibrium response becomes

$$B_1\Delta T_1 + B_2\Delta T_2 = \Delta A_1 + \Delta A_2 = \Delta A, \tag{25}$$

where ΔA_1 and ΔA_2 are heat perturbations in the extratropics and tropics, respectively, which can result from changes in solar radiation, OLR at the TOA, and planetary albedo, because of, for example, sea ice change in the polar region, deep convection in the tropics, or greenhouse gases. The responses of local and global mean temperatures can be written in terms of ΔT_s as follows:

$$\Delta T_1 = \frac{\Delta A - B_2\Delta T_s}{B_1 + B_2}, \quad \Delta T_2 = \frac{\Delta A + B_1\Delta T_s}{B_1 + B_2}, \quad \text{and}$$
$$\Delta T_m = \frac{\Delta A + (B_1 - B_2)\Delta T_s/2}{B_1 + B_2}. \tag{26}$$

Now, the corresponding changes in heat transport components are

$$\Delta F_o = \Delta F_t - \Delta F_a = G_{01}\frac{B_1\Delta A_2 - B_2\Delta A_1 - [B_1B_2 + (B_1 + B_2)\chi]\Delta T_s}{B_1 + B_2}, \tag{27a}$$

$$\Delta F_a = \chi G_{01}\Delta T_s, \quad \text{and} \tag{27b}$$

$$\Delta F_t = G_{01}\frac{B_1\Delta A_2 - B_2\Delta A_1 - B_1B_2\Delta T_s}{B_1 + B_2}. \tag{27c}$$

The ratio between the changes in AHT and OHT is

$$C_h \equiv \frac{\Delta F_a}{\Delta F_o} = -\frac{(B_1 + B_2)\chi}{[B_1B_2 + (B_1 + B_2)\chi] + (B_2\Delta A_1 - B_1\Delta A_2)/\Delta T_s} = \left[\frac{1}{1 + \dfrac{(B_2\Delta A_1 - B_1\Delta A_2)/\Delta T_s}{B_1B_2 + (B_1 + B_2)\chi}}\right] C_R, \tag{28}$$

which suggests a big uncertainty to the BJC due to external heating. In fact, Eqs. (25), (27), and (28) can be

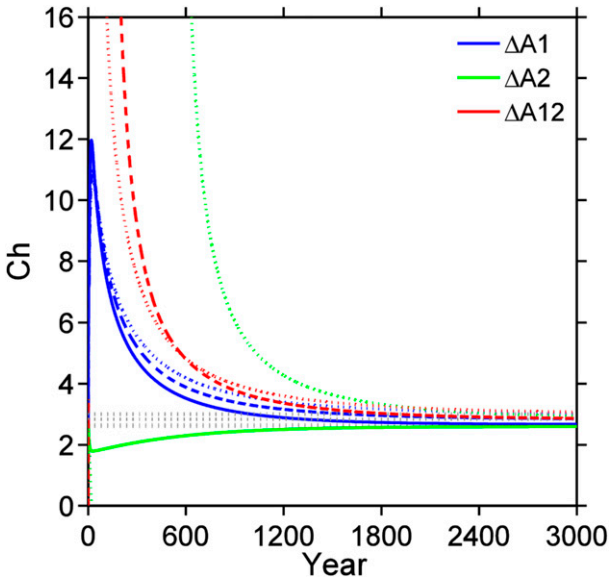

FIG. 5. Ratio of anomalous AHT to anomalous OHT in the heat perturbation experiments. Different colors show ratios for different regional forcing. Dotted gray lines show the ratios based on the analytical solution of Eq. (28). Blue curves are for the cases that the heat perturbation is only added to ocean box 1 ($\Delta A_1 = 3.2\,\mathrm{W\,m^{-2}}$, $\Delta A_2 = 0$). Green curves are for the cases that the heat perturbation is only added to ocean box 2 ($\Delta A_1 = 0$, $\Delta A_2 = 3.2\,\mathrm{W\,m^{-2}}$). Red curves are for the cases that the heat perturbation is added to both boxes 1 and 2 ($\Delta A_1 = \Delta A_2 = 3.2\,\mathrm{W\,m^{-2}}$). Curves correspond to the three different feedback situations of FB1 (solid), FB2 (dashed), and FB3 (dotted). The cases FB1, FB2, and FB3 are defined in the caption of Fig. 2.

reduced to Eqs. (16)–(18) when neglecting the heat perturbation ΔA. Equation (28) shows that the pattern and amplitude of external forcing, as well as the climate response ΔT_s itself, could all affect the BJC rate. This is dramatically different from the BJC in Eq. (18) under freshwater perturbation, which shows clearly that it depends only on internal climate parameters.

A series of heat perturbation experiments are performed, with a reasonable amount of heat added in the extratropics ($\Delta A_1 > 0$ and $\Delta A_2 = 0$), the tropics ($\Delta A_1 = 0$ and $\Delta A_2 > 0$), or both ($\Delta A_1 > 0$ and $\Delta A_2 > 0$). Here, our only concern is the stable climate, which requires that the heat perturbation should not be too strong. In addition, the same feedback parameters as those in the freshwater perturbation experiments are used. No positive feedback in the tropics ($-B_2 > 0$) is considered in the heating experiments to prevent the model climate from running away.

No BJC is found in the heating experiments (Fig. 5). Instead, the changes in AHT and OHT are always in phase, and the change in AHT is always larger than that in OHT ($C_h > 1$). Figure 5 shows the transient change of $C_h(\Delta F_a/\Delta F_o)$ (colored curves) and C_h based on Eq. (28) (dotted gray lines) under different regional forcing and different feedback situations. No matter how different the transient behaviors of C_h are, the equilibrium C_h always tends to reach a constant. However, Eq. (28) also suggests that C_h could be equal to C_R if $B_2A_1 = B_1\Delta A_2$. For example, in the cases of tropical heat perturbation ($\Delta A_1 = 0$ and $\Delta A_2 > 0$) with $B_1 = 0$ and global uniform heat perturbation ($\Delta A_1 = \Delta A_2 > 0$) with uniform feedback $B_1 = B_2$, the BJC should exist ($C_h = C_R$). Yet, in our experiments, C_h is eventually larger than zero, because $\Delta T_s = 0$ in these two cases (these two curves are not shown in Fig. 5).

The surface salinity changes can be eventually neglected (Fig. 6a) in all heating experiments, no matter what the patterns of forcing and feedbacks are. The change in mass transport q (Fig. 6c) is thus determined only by the temperature change (Fig. 6b). Figure 6a shows the maximum S_s change of 0.06 psu, less than 0.2% of the reference salinity (35 psu), under global uniform heating ($\Delta A_1 = \Delta A_2 > 3.2\,\mathrm{W\,m^{-2}}$) with extratropical positive feedback ($-B_1 = 0.3$). Under the same forcing, the T_s change is significant (about −3°C) (Fig. 6b), determining the THC change (Fig. 6c). The changes in AHT and OHT are therefore of the same sign, because they are similarly determined by T_s, no matter where the heat is added, and are also independent of detailed climate feedbacks.

The heat perturbation experiments show that the BJC between AHT and OHT would never happen because of the violation of global total energy conservation [Eq. (25)]. It is worth noting that, although the analytical solution of Eq. (28) suggests big uncertainty in C_h, the actual rate is roughly certain, because the role of salinity in the THC is negligible. This can be better understood by further simplifying the box model.

Suppose q in Eq. (3) is only determined by ocean temperature, and the dynamic feedback between q and S_s is cut off. Mathematically, the equilibrium rate C_h in Eq. (28) can be reduced to the following:

$$C_h \equiv \frac{\Delta F_a}{\Delta F_o} \simeq \frac{\chi}{2\epsilon c\kappa\alpha\rho_0 D_1 T_s} = \frac{1}{2}\frac{F_a}{F_o} > 0. \qquad (29)$$

Here, $q = \kappa\alpha T_s$. If we assume a constant $q = q_0$, the ratio in Eq. (29) can be further simplified to

$$C_h \equiv \frac{\Delta F_a}{\Delta F_o} = \frac{\chi}{\epsilon c\rho_0 D_1 q_0} = \frac{F_a}{F_o} > 0. \qquad (30)$$

This explicitly shows that the changes in AHT and OHT are of the same sign and are eventually determined by the ratio of mean AHT and mean OHT if no salinity is involved in the mass transport. A change in S_s cannot affect T_s, q, F_a, and F_o, and there will be no so-called BJC. A change in T_s cannot affect S_s either, but q, F_a,

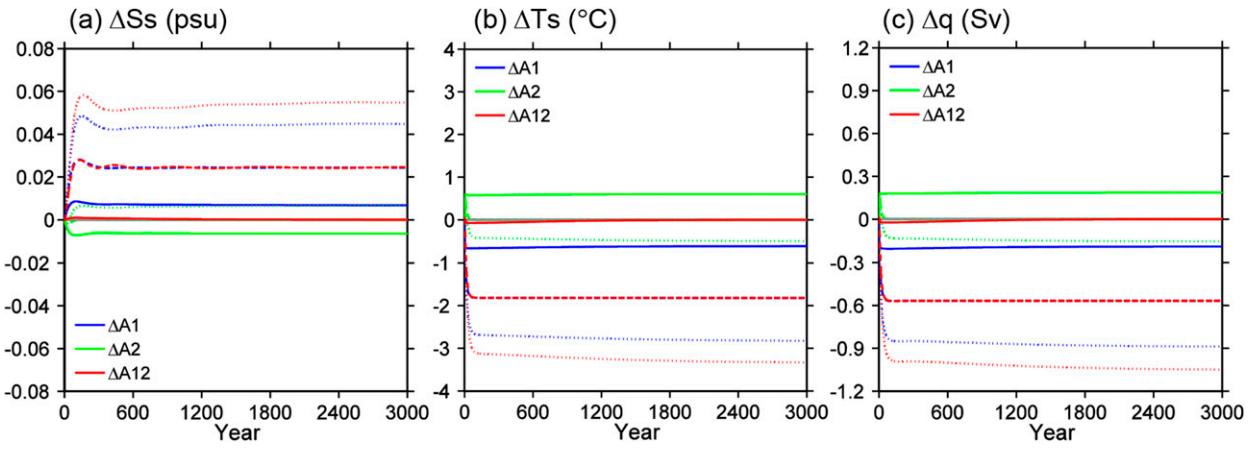

FIG. 6. Changes in (a) S_s (psu), (b) T_s (°C), and (c) mass transport q (Sv) in the heat perturbation experiments. As in Fig. 5, different colors are for different regional forcing; and curves are for the three different feedback situations of FB1 (solid), FB2 (dashed), and FB3 (dotted). The cases FB1, FB2, and FB3 are defined in the caption of Fig. 2.

and F_o will change proportionally with T_s. Equation (29) is still valid, but the BJC is not possible. This implies a critical role of salinity in the occurrence of BJC in the climate system.

A series of parallel heat perturbation experiments (similar to Fig. 5) with $q = \kappa\alpha T_s$ are performed to examine Eqs. (28) and (29). Figure 7 shows transient changes of C_h ($=\Delta F_a/\Delta F_o$) (red curves) and C_h based on Eq. (29) (dotted red lines). The curves of C_h in Fig. 5 are also plotted in Fig. 7 (as blue curves and dotted gray lines) for comparison. The difference between Eqs. (28) and (29) is within 5% of the mean C_h, regardless of the strength of surface heat perturbation or feedbacks. The equilibrium ratio C_h approaches the values suggested by Eq. (29). Equation (29) provides an easier and more practical way of scaling the relative changes in AHT and OHT under heat perturbation.

c. *BJC under both freshwater forcing and heat forcing*

What will happen to the BJC when both external freshwater and heat fluxes are considered simultaneously in the coupled box model? A number of sensitivity experiments are performed in which the freshwater hosing varies gradually from 0 to −0.5 Sv; at the same time, the heat forcing changes from 0 to $-5\,\mathrm{W\,m^{-2}}$. To guarantee a stable climate, we study the situations when a cooling occurs in the extratropics and freshwater is removed there as well. This consideration agrees with the common intuitionistic concept on climate change: a global cooling (warming) is usually accompanied by sea ice formation (melting) and thus increases (decreases) ocean salinity in the polar oceans. In addition, in these experiments weak positive (strong negative) feedback is assumed in the extratropics (tropics) ($-B_1 = 0.3$ and $-B_2 = -1.7$). The other parameters are the same as those in Table 1.

Figure 8a shows a summary of the BJC. The yellow shaded region shows where the BJC is valid. First, in the extreme case without external heating, the BJC is a constant (−1.3), independent of the magnitude of freshwater flux. Second, in another extreme case without external freshwater, the BJC is also near a constant (2.6), roughly equal to the value given by Eq. (29) and consistent with Figs. 5 and 7. Third, even a small amount of external heat forcing will result in a complete failure of the BJC. It shows that stronger freshwater perturbation can delay the BJC failure to some extent (Fig. 8a).

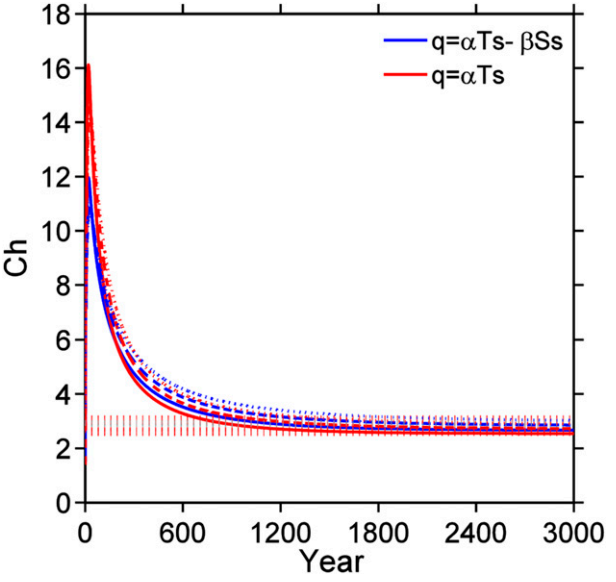

FIG. 7. As in Fig. 5, but for the ratio when $q = \alpha T_s$ (red curves). The heat perturbation experiments are similar to those shown in Fig. 5 (the blue curves, which are also plotted here for comparison). Dotted red lines show the ratios based on the analytical solution of Eq. (29).

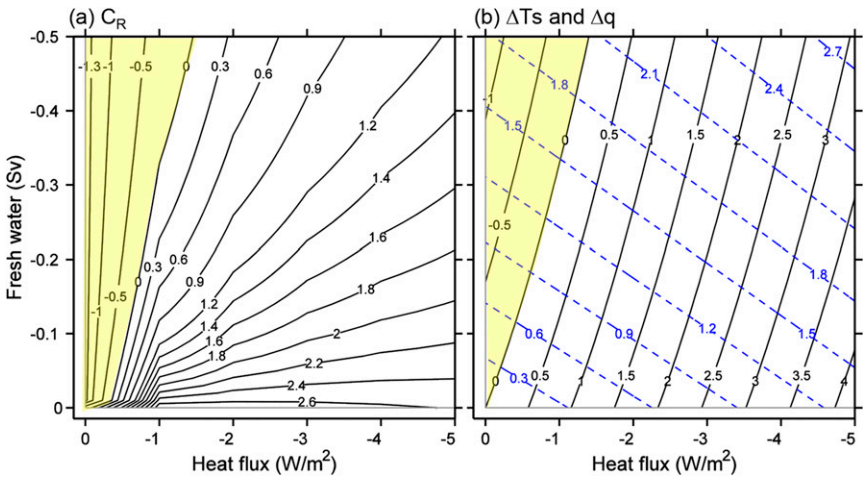

FIG. 8. (a) BJC rate (C_R) with respect to surface heat flux forcing and freshwater forcing. The local feedback parameters are $-B_1 = 0.3$ and $-B_2 = -1.7$. (b) As in (a), but for changes in T_s (black solid curves; °C) and in mass transport q (blue dashed curves; Sv). The yellow shaded region in each panel shows the region where the BJC occurs.

With heat perturbation, the changes in AHT and OHT will not compensate each other in most situations. The mechanism for the valid (invalid) BJC is given in Fig. 8b. In the yellow shaded region, T_s change is determined by THC change, which in turn is determined by the salinity change in response to freshwater forcing. Removing freshwater in the extratropical ocean causes an intensified THC ($\Delta F_o > 0$), resulting in a warming in the extratropics and thus the weakening of T_s ($\Delta T_s < 0$, so $\Delta F_a < 0$). Since the external heating is weak in the yellow shaded region, it does not affect T_s too much. Outside the yellow shaded region, the external heating dominates the THC effect on the T_s change, which results in in-phase changes in AHT and OHT ($\Delta F_a \propto \Delta T_s$ and $\Delta F_o \propto \Delta T_s$) and the failure of BJC finally.

The conceptual box model might exaggerate the effect of heat perturbation or distort effects of both heat and freshwater perturbations on heat transports because of its simplicity. However, these sensitivity experiments show conceptually that the BJC can fail easily if global total energy imbalance happens. The accumulated heat imbalance due to CO_2 change since the last glacial maximum (LGM) is about 3.3 W m^{-2} (Shakun et al. 2012). This corresponds to a yearly heat perturbation of about 1.5×10^{-4} W m^{-2}. Over such a long period, its effect on the MHT is negligible when compared with the freshwater effect, so the BJC is still valid during the past 22 000 yr (Yang et al. 2015). However, the accumulated CO_2-related heat imbalance since the preindustrial is around 1.66 ± 0.17 W m^{-2}, or around 1×10^{-2} W m^{-2} yearly (IPCC 2007). Whether the BJC is valid during this shorter period needs to be investigated thoroughly. Additional experiments were performed to examine the robustness of Fig. 8a. In these experiments, the local feedback parameters were given different values, and global warming and freshening were considered. The conclusions from these experiments are qualitatively unchanged: if the heat perturbation dominates the freshwater perturbation in determining surface temperature change, the BJC will hardly occur, because the global total energy conservation is violated.

4. Summary and discussion

This study investigates the BJC using a coupled box model. The model mean climate was tuned to resemble Earth's current climate, which is in the regime of a stable equilibrium state with a strong (weak) meridional temperature (salinity) gradient. The BJC was derived analytically. Under the assumptions in the box model, we found the BJC rate is independent of the heat transports themselves and is determined only by two internal climate parameters: the local climate feedback between temperature and the energy flux at the TOA and the AHT efficiency.

Energy conservation is the intrinsic mechanism of the BJC, as shown in Fig. 4. To see how the BJC would happen, perturbation experiments were performed. Under freshwater perturbation, the total energy of the model system remained undisturbed. The atmosphere will always compensate the OHT change, and thus the BJC is always valid. The BJC can exhibit three different behaviors, depending on the climate feedback. In the case of global negative feedback, the atmosphere tends to undercompensate the OHT change. Stronger local

negative feedback will result in a lower compensation rate, because stronger negative feedback helps to fulfil the energy balance more locally through vertical processes rather than via horizontal redistribution. In the case of weak local positive feedback somewhere, the atmosphere will overcompensate the OHT change, because positive feedback tends to amplify the initial heat imbalance caused by OHT perturbation, and the atmosphere has to import (export) extra energy to make up for the extra local energy loss (gain). The stronger local positive feedback will result in bigger overcompensation. In the case of zero feedback somewhere, the atmosphere will compensate the OHT change perfectly, because zero feedback means zero heat imbalances at the TOA, and any heat imbalance caused by OHT perturbation has to be fully offset horizontally via AHT. In any of these cases, a higher AHT efficiency helps to reach a better compensation.

No BJC was found when perturbing the climate with external heat forcing only, because the global total energy conservation is violated so that the changes in AHT and OHT do not have to compensate. Instead, they are always in phases in the heating experiments, and the anomalous AHT is always larger than the anomalous OHT ($C_h > 1$). In this case, the change in mass transport is predominantly determined by temperature change. The changes in AHT and OHT are therefore of the same sign, because they are similarly determined by T_s. It is interesting to see that, under the assumptions in the coupled box model, the equilibrium C_h always tends to approach the constant suggested by Eq. (29) and appears to be insensitive to the location, amplitude, and pattern of heat perturbation.

The BJC appears to imply a fundamental mechanism that constrains the global climate change. The out-of-phase changes in AHT and OHT, as well as in the tropical and extratropical regions, assure a small change in the global climate. This mechanism can be crucial to Earth's overall climate stability. It may shed light on a potential self-restoring mechanism in a complex climate system. However, we are experiencing with the present Earth climate rising global mean temperature and sea ice melting; whether the BJC is working in reality is a serious concern to us. The coupled box model shows that the BJC is very sensitive to external heat forcing. The BJC, however, does not rule out remarkable local climate change or individual change in ocean or atmosphere (NSM94). Our investigation on the BJC in an earth system model under CO_2 forcing is on the way.

The coupled box model with a four-box ocean can have the same mean climate as the coupled box model of a two-box ocean (MS95) under the same key parameters. However, our coupled box model has an explicit THC dynamics and is more appropriate for studying the response time scale and the transient behavior of the BJC. At what time scale the BJC will be valid is another important issue on which we are working. The BJC suggests a strong negative correlation between AHT and OHT. Our ongoing study focuses on the question of whether this negative correlation suggests a strong negative feedback in the climate system.

We are fully aware of the limitations of the coupled box model. For example, under the assumptions in the coupled box model, the BJC is independent of the heat transports themselves. Rose and Ferreira (2013) showed that this independence failed to capture the range of behaviors suggested in a complex GCM. The AHT and moisture transport were parameterized to be linearly determined by T_s. This is appropriate for the atmosphere in mid and high latitudes and is derived from the baroclinic stability theory (Stone and Yao 1990; NSM94). However, in the tropics the AHT is mainly accomplished by mean circulation, such as the Hadley cells. The model is constructed based on a Stommel-like hemispheric box model and includes only a buoyancy-driven overturning circulation. In reality, there is no well-defined equator-to-pole-scale overturning circulation. There is substantial wind-driven heat transport in a real ocean basin, which is missing in the coupled box model because it does not include any wind-driven dynamics. Even the overturning circulation is assumed to depend indirectly on wind-driven mixing in the Southern Ocean (e.g., Toggweiler and Samuels 1995, 1998). Nevertheless, the simple coupled box model can help us understand the fundamental mechanisms of the BJC. To what extent these fundamental mechanisms exist in reality has to be examined in a complex coupled climate model.

Acknowledgments. We thank three reviewers for their critical comments on earlier versions of the paper and for providing some references. This work is jointly supported by the NSF of China (41376007, 41176002, 91337106, and 40976007) and the National Basic Research Program of China (2012CB955200).

REFERENCES

Abbot, D. S., and E. Tziperman, 2008: A high-latitude convective cloud feedback and equable climates. *Quart. J. Roy. Meteor. Soc.*, **134**, 165–185, doi:10.1002/qj.211.

Bates, J. R., 1999: A dynamical stabilizer in the climate system: A mechanism suggested by a simple model. *Tellus*, **51A**, 349–372, doi:10.1034/j.1600-0870.1999.t01-3-00002.x.

——, 2007: Some considerations of the concept of climate feedback. *Quart. J. Roy. Meteor. Soc.*, **133**, 545–560, doi:10.1002/qj.62.

——, 2012: Climate stability and sensitivity in some simple conceptual models. *Climate Dyn.*, **38**, 455–473, doi:10.1007/s00382-010-0966-0.

Bjerknes, J., 1964: Atlantic air–sea interaction. *Advances in Geophysics*, Vol. 10, Academic Press, 1–82.

Budyko, M. I., 1969: The effect of solar radiation variations on the climate of the Earth. *Tellus*, **21A**, 611–619, doi:10.1111/j.2153-3490.1969.tb00466.x.

Carton, J. A., and B. Giese, 2008: A reanalysis of ocean climate using Simple Ocean Data Assimilation (SODA). *Mon. Wea. Rev.*, **136**, 2999–3017, doi:10.1175/2007MWR1978.1.

Cheng, W., C. M. Bitz, and J. C. H. Chiang, 2007: Adjustment of the global climate to an abrupt slowdown of the Atlantic meridional overturning circulation. *Ocean Circulation: Mechanisms and Impacts*, *Geophys. Monogr.*, Vol. 173, Amer. Geophys. Union, 295–313.

Clement, A. C., R. Burgman, and J. R. Norris, 2009: Observational and model evidence for positive low-level cloud feedback. *Science*, **325**, 460–464, doi:10.1126/science.1171255.

Donohoe, A., J. Marshall, D. Ferreira, and D. Mcgee, 2013: The relationship between ITCZ location and cross-equatorial atmospheric heat transport: From the seasonal cycle to the Last Glacial Maximum. *J. Climate*, **26**, 3597–3618, doi:10.1175/JCLI-D-12-00467.1.

Enderton, D., and J. Marshall, 2009: Explorations of atmosphere–ocean–ice climates on an aquaplanet and their meridional energy transports. *J. Atmos. Sci.*, **66**, 1593–1611, doi:10.1175/2008JAS2680.1.

Farneti, R., and G. Vallis, 2013: Meridional energy transport in the coupled atmosphere–ocean system: Compensation and partitioning. *J. Climate*, **26**, 7151–7166, doi:10.1175/JCLI-D-12-00133.1.

Feldl, N., and G. H. Roe, 2013a: The nonlinear and nonlocal nature of climate feedbacks. *J. Climate*, **26**, 8289–8304, doi:10.1175/JCLI-D-12-00631.1.

——, and ——, 2013b: Four perspectives on climate feedbacks. *Geophys. Res. Lett.*, **40**, 4007–4011, doi:10.1002/grl.50711.

Frierson, D. M., and Y.-T. Huang, 2012: Extratropical Influence on ITCZ shifts in slab ocean simulations of global warming. *J. Climate*, **25**, 720–733, doi:10.1175/JCLI-D-11-00116.1.

Herweijer, C., R. Seager, M. Winton, and A. Clement, 2005: Why ocean heat transport warms the global mean climate. *Tellus*, **57A**, 662–675, doi:10.1111/j.1600-0870.2005.00121.x.

Huang, R. X., J. R. Luyten, and H. M. Stommel, 1992: Multiple equilibrium states in combined thermal and saline circulation. *J. Phys. Oceanogr.*, **22**, 231–246, doi:10.1175/1520-0485(1992)022<0231:MESICT>2.0.CO;2.

Huang, Y., and M. Zhang, 2014: The implication of radiative forcing and feedback for meridional energy transport. *Geophys. Res. Lett.*, **41**, 1665–1672, doi:10.1002/2013GL059079.

Huber, M., and R. Caballero, 2011: The early Eocene equable climate problem revisited. *Climate Past*, **7**, 603–633, doi:10.5194/cp-7-603-2011.

Hughes, T. C. M., and A. J. Weaver, 1994: Multiple equilibria of an asymmetric two-basin model. *J. Phys. Oceanogr.*, **24**, 619–637, doi:10.1175/1520-0485(1994)024<0619:MEOAAT>2.0.CO;2.

Hwang, Y. T., and D. M. Frierson, 2010: Increasing atmospheric poleward energy transport with global warming. *Geophys. Res. Lett.*, **37**, L24807, doi:10.1029/2010GL045440.

——, ——, and J. E. Kay, 2011: Coupling between Arctic feedbacks and changes in poleward energy transport. *Geophys. Res. Lett.*, **38**, L17704, doi:10.1029/2011GL048546.

IPCC, 2007: Summary for Policymakers. *Climate Change 2007: The Physical Science Basis*, S. Solomon et al., Eds., Cambridge University Press, 1–18. [Available online at https://www.ipcc.ch/pdf/assessment-report/ar4/wg1/ar4-wg1-spm.pdf.]

Kang, S. M., I. M. Held, D. M. W. Frierson, and M. Zhao, 2008: The response of the ITCZ to extratropical thermal forcing: Idealized slab-ocean experiments with a GCM. *J. Climate*, **21**, 3521–3532, doi:10.1175/2007JCLI2146.1.

——, D. M. W. Frierson, and I. M. Held, 2009: The tropical response to extratropical thermal forcing in an idealized GCM: The importance of radiative feedbacks and convective parameterization. *J. Atmos. Sci.*, **66**, 2812–2827, doi:10.1175/2009JAS2924.1.

Langen, P. L., and V. A. Alexeev, 2007: Polar amplification as a preferred response in an idealized aquaplanet GCM. *Climate Dyn.*, **29**, 305–317, doi:10.1007/s00382-006-0221-x.

Lindzen, R. S., and B. Farrell, 1977: Some realistic modifications of simple climate models. *J. Atmos. Sci.*, **34**, 1487–1501, doi:10.1175/1520-0469(1977)034<1487:SRMOSC>2.0.CO;2.

Liu, Z., H. Yang, C. He, and Y. Zhao, 2015: A theory for Bjerknes compensation: The role of climate feedback. *J. Climate*, doi:10.1175/JCLI-D-15-0227.1, in press.

Manabe, S., and R. J. Stouffer, 1995: Simulation of abrupt climate change induced by freshwater input to the North Atlantic Ocean. *Nature*, **378**, 165–167, doi:10.1038/378165a0.

Marotzke, J., 1990: Instabilities and multiple equilibria of the thermohaline circulation. Ph.D. thesis, Institut für Meereskunde, 126 pp.

——, and P. Stone, 1995: Atmospheric transports, the thermohaline circulation, and flux adjustments in a simple coupled model. *J. Phys. Oceanogr.*, **25**, 1350–1364, doi:10.1175/1520-0485(1995)025<1350:ATTTCA>2.0.CO;2.

Nakamura, M., P. H. Stone, and J. Marotzke, 1994: Destabilization of the thermohaline circulation by atmospheric eddy transports. *J. Climate*, **7**, 1870–1882, doi:10.1175/1520-0442(1994)007<1870:DOTTCB>2.0.CO;2.

North, G. R., 1975: Theory of energy-balance climate models. *J. Atmos. Sci.*, **32**, 2033–2043, doi:10.1175/1520-0469(1975)032<2033:TOEBCM>2.0.CO;2.

——, 1984: The small ice cap instability in diffusive climate models. *J. Atmos. Sci.*, **41**, 3390–3395, doi:10.1175/1520-0469(1984)041<3390:TSICII>2.0.CO;2.

Philander, S. G. H., D. Gu, D. Halpern, G. Lambert, N.-C. Lau, T. Li, and R. C. Pancanowiski, 1996: Why the ITCZ is mostly north of the equator. *J. Climate*, **9**, 2958–2972, doi:10.1175/1520-0442(1996)009<2958:WTIIMN>2.0.CO;2.

Pierrehumbert, R., 1995: Thermostats, radiator fins, and the local runaway greenhouse. *J. Atmos. Sci.*, **52**, 1784–1805, doi:10.1175/1520-0469(1995)052<1784:TRFATL>2.0.CO;2.

Rayner, N. A., D. E. Parker, E. B. Horton, C. K. Folland, L. V. Alexander, D. P. Rowell, E. C. Kent, and A. Kaplan, 2003: Global analyses of sea surface temperature, sea ice, and night marine air temperature since the late nineteenth century. *J. Geophys. Res.*, **108**, 4407, doi:10.1029/2002JD002670.

Rose, B. E., and J. Marshall, 2009: Ocean heat transport, sea ice, and multiple climate states: Insights from energy balance models. *J. Atmos. Sci.*, **66**, 2828–2843, doi:10.1175/2009JAS3039.1.

——, and D. Ferreira, 2013: Ocean heat transport and water vapor greenhouse in a warm equable climate: A new look at the low gradient paradox. *J. Climate*, **26**, 2117–2136, doi:10.1175/JCLI-D-11-00547.1.

——, K. C. Armour, D. S. Battisti, N. Feldl, and D. D. Koll, 2014: The dependence of transient climate sensitivity and radiative feedbacks on the spatial pattern of ocean heat uptake. *Geophys. Res. Lett.*, **41**, 1071–1078, doi:10.1002/2013GL058955.

Seo, J., S. M. Kang, and D. M. Frierson, 2014: Sensitivity of intertropical convergence zone movement to the latitudinal position of thermal forcing. *J. Climate*, **27**, 3035–3042, doi:10.1175/JCLI-D-13-00691.1.

Shaffrey, L., and R. Sutton, 2006: Bjerknes compensation and the decadal variability of the energy transports in a coupled climate model. *J. Climate*, **19**, 1167–1181, doi:10.1175/JCLI3652.1.

Shakun, J. D., and Coauthors, 2012: Global warming preceded by increasing carbon dioxide concentrations during the last deglaciation. *Nature*, **484**, 49–54, doi:10.1038/nature10915.

Soden, B. J., A. J. Broccoli, and R. S. Hemler, 2004: On the use of cloud forcing to estimate cloud feedback. *J. Climate*, **17**, 3661–3665, doi:10.1175/1520-0442(2004)017<3661:OTUOCF>2.0.CO;2.

Stommel, H., 1961: Thermohaline convection with two stable regimes of flow. *Tellus*, **13A**, 224–230, doi:10.1111/j.2153-3490.1961.tb00079.x.

Stone, P. H., 1978: Constraints on dynamical transports of energy on a spherical planet. *Dyn. Atmos. Oceans*, **2**, 123–139, doi:10.1016/0377-0265(78)90006-4.

——, and M.-S. Yao, 1990: Development of a two-dimensional zonally averaged statistical–dynamical model. Part III: The parameterization of the eddy fluxes of heat and moisture. *J. Climate*, **3**, 726–740, doi:10.1175/1520-0442(1990)003<0726:DOATDZ>2.0.CO;2.

Stouffer, R. J., D. Seidov, and B. J. Haupt, 2007: Climate response to external sources of freshwater: North Atlantic versus the Southern Ocean. *J. Climate*, **20**, 436–448, doi:10.1175/JCLI4015.1.

Toggweiler, J. R., and B. Samuels, 1995: Effect of drake passage on the global thermohaline circulation. *Deep-Sea Res. I*, **42**, 477–500, doi:10.1016/0967-0637(95)00012-U.

——, and ——, 1998: On the ocean's large-scale circulation near the limit of no vertical mixing. *J. Phys. Oceanogr.*, **28**, 1832–1852, doi:10.1175/1520-0485(1998)028<1832:OTOSLS>2.0.CO;2.

Trenberth, K. E., and J. M. Caron, 2001: Estimates of meridional atmosphere and ocean heat transports. *J. Climate*, **14**, 3433–3443, doi:10.1175/1520-0442(2001)014<3433:EOMAAO>2.0.CO;2.

Tziperman, E., J. R. Toggweiler, Y. Feliks, and K. Bryan, 1994: Instability of the thermohaline circulation with respect to mixed boundary conditions: Is it really a problem for realistic models? *J. Phys. Oceanogr.*, **24**, 217–232, doi:10.1175/1520-0485(1994)024<0217:IOTTCW>2.0.CO;2.

Vallis, G. K., and R. Farneti, 2009: Meridional energy transport in the coupled atmosphere–ocean system: Scaling and numerical experiments. *Quart. J. Roy. Meteor. Soc.*, **135**, 1643–1660, doi:10.1002/qj.498.

Van der Swaluw, E., S. S. Drijfhout, and W. Hazeleger, 2007: Bjerknes compensation at high northern latitudes: The ocean forcing the atmosphere. *J. Climate*, **20**, 6023–6032, doi:10.1175/2007JCLI1562.1.

Vellinga, M., and P. Wu, 2008: Relations between northward ocean and atmosphere energy transports in a coupled climate model. *J. Climate*, **21**, 561–575, doi:10.1175/2007JCLI1754.1.

Wang, W.-C., and P. H. Stone, 1980: Effect of ice–albedo feedback on global sensitivity in a one-dimensional radiative–convective climate model. *J. Atmos. Sci.*, **37**, 545–552, doi:10.1175/1520-0469(1980)037<0545:EOIAFO>2.0.CO;2.

Yang, H., and H. Dai, 2014: Effect of wind forcing on the meridional heat transport in a coupled climate model: Equilibrium response. *Climate Dyn.*, **45**, 1451–1470, doi:10.1007/s00382-014-2393-0.

——, Y. Wang, and Z. Liu, 2013: A modelling study of the Bjerknes compensation in the meridional heat transport in a freshening ocean. *Tellus*, **65A**, 18480, doi:10.3402/tellusa.v65i0.18480.

——, Y. Zhao, Z. Liu, Q. Li, F. He, and Q. Zhang, 2015: Heat transport compensation in atmosphere and ocean over the past 22,000 years. *Nat. Sci. Rep.*, **5**, 16661, doi:10.1038/srep16661.

Zelinka, M. D., and D. L. Hartmann, 2011: The observed sensitivity of high clouds to mean surface temperature anomalies in the tropics. *J. Geophys. Res.*, **116**, D23103, doi:10.1029/2011JD016459.

——, and ——, 2012: Climate feedbacks and their implications for poleward energy flux changes in a warming climate. *J. Climate*, **25**, 608–624, doi:10.1175/JCLI-D-11-00096.1.

Zhang, M., J. Hack, J. Kiehl, and R. Cess, 1994: Diagnostic study of climate feedback processes in atmospheric general circulation models. *J. Geophys. Res.*, **99**, 5525–5537, doi:10.1029/93JD03523.

Zhang, R., and T. Delworth, 2005: Simulated tropical response to a substantial weakening of the Atlantic thermohaline circulation. *J. Climate*, **18**, 1853–1860, doi:10.1175/JCLI3460.1.

——, S. M. Kang, and I. M. Held, 2010: Sensitivity of climate change induced by weakening of the Atlantic meridional overturning circulation to cloud feedback. *J. Climate*, **23**, 378–389, doi:10.1175/2009JCLI3118.1.